


Fenoldopam Mesylate Enhances the Survival of Mesenchymal Stem Cells Under Oxidative Stress and Increases the Therapeutic Function in Acute Kidney Injury

Cell Transplantation
Volume 32: 1–13
© The Author(s) 2023
Article reuse guidelines:
sagepub.com/journals-permissions
DOI: 10.1177/09636897221147920
journals.sagepub.com/home/cll


Seo Yeon Jo¹, Hye Jin Cho¹ , and Tae Min Kim^{1,2} 

Abstract

Mesenchymal stem cells (MSCs) have gained interest as an alternative therapeutic option for renal diseases, including acute kidney injury (AKI). However, their use is often limited owing to low survival rates *in vivo*. Fenoldopam mesylate (FD) is a selective dopamine D1 receptor agonist with antioxidative and anti-apoptotic roles. Herein, we investigated whether FD can enhance the survival of MSCs undergoing oxidative stress *in vitro*. In addition, the therapeutic effect of MSCs and FD-treated MSCs (FD-MSCs) was compared in a mouse model of AKI induced by cisplatin. The survival of MSCs under oxidative stress was augmented by FD treatment. FD induced the phosphorylation of cAMP response element-binding protein and AKT, contributing to enhanced growth compared with untreated MSCs. The expression of nuclear factor erythroid-2-related factor 2 (NRF2) and heme oxygenase-1 was increased by FD treatment, and nuclear translocation of NRF2 was found exclusively in FD-MSCs. FD downregulated BAX expression, increased the mitochondrial membrane potential, reduced reactive oxygen species generation, and decreased the apoptotic death of MSCs induced by oxidative stress. Moreover, renal function and tubular injury were improved in FD-MSCs compared with non-treated MSCs. Furthermore, tubular injury, apoptosis, and macrophage infiltration, as well as the serum level of tumor necrosis factor- α were reduced, while tubular cell proliferation was markedly increased in FD-MSCs compared with MSCs. Our study demonstrated that FD increases the survivability of MSCs in an oxidative environment, and its use may be effective in preparing robust therapeutic MSCs.

Keywords

mesenchymal stem cells, dopamine D1 receptor, fenoldopam mesylate, oxidative stress, acute kidney injury

Introduction

Acute kidney injury (AKI) is a condition in which kidney function rapidly deteriorates within hours to days, and it remains a major global health problem that leads to high mortality and morbidity¹. According to a worldwide meta-analysis in 2013 based on the Kidney Disease Improving Global Outcome (KDIGO), the overall AKI-associated mortality rate is 23%². Furthermore, episodes of AKI increase the risk of chronic renal failure and end-stage renal disease (ESRD)^{3,4}. Current treatment for AKI includes hemodynamic control using fluids, diuretics, dopamine, a calcium channel inhibitor, and a renin-angiotensin system (RAS) inhibitor⁵. Currently, no single drug can be used for AKI due to its complex pathophysiology⁵. Moreover, it has been suggested that the current therapeutic protocol is not adequate due to the lack of a strategy that can enhance the regeneration of renal parenchymal cells⁶.

During the past decade, growing evidence has shown that mesenchymal stem cells (MSCs) have therapeutic potential in degenerative diseases, including AKI^{7–9}. MSCs release extracellular vesicles and other active biomolecules including growth factors and cytokines, which all can stimulate the

¹ Graduate School of International Agricultural Technology, Seoul National University, Pyeongchang, South Korea

² Institutes of Green Bio Science & Technology, Seoul National University, Pyeongchang, South Korea

Submitted: May 9, 2022. Revised: December 5, 2022. Accepted: December 9, 2022.

Corresponding Author:

Tae Min Kim, Graduate School of International Agricultural Technology and Institutes of Green Bio Science & Technology, Seoul National University, Pyeongchang Daero 1447, Pyeongchang 25354, Gangwon-do, South Korea.

Email: taemin21@snu.ac.kr



recovery of injured tissue¹⁰. The expression of major histocompatibility complex antigens in MSCs is relatively low, making them implantable and increasing their potential clinical uses¹¹. However, their therapeutic efficacy varies, often resulting in inconsistent outcomes¹². Particularly, transplanted cells encounter stressful situations such as low oxygen, restricted nutrient supply, and oxidative stress^{10,13}, resulting in reduced proliferation, loss of stemness, and senescence¹⁴. Thus, attempts have been made to enhance the survival or therapeutic efficacy of MSCs by improving survival or migration via culture condition optimization, genetic engineering, or treatment with cytokines or small molecules^{15–17}.

Oxidative stress can be defined as a serious disturbance of the balance between the production and removal of pro-oxidants or free radicals, which oxidize lipids, proteins, and DNA, and detoxification ability¹⁸. Several dopamine receptors, including D1, D2, and D5, have been shown to be important for maintaining a normal redox balance¹⁹. Fenoldopam mesylate (FD) is the first selective dopamine D1 receptor agonist approved for clinical use²⁰. In cell-based studies, a low concentration of dopamine D1 agonists has been demonstrated to have antioxidant effects in diverse cells^{21–24}. For example, a dopamine D1 agonist reduces platelet-derived growth factor-beta-induced oxidative stress via activation of protein kinase A in vascular smooth muscle cells²¹. Another report showed that the D1 receptor is involved in decreasing reduced nicotinamide adenine dinucleotide phosphate oxidase activity, thereby lowering oxidative stress in renal tubular cells²².

Here, we investigated whether FD can increase the survival of MSCs undergoing oxidative stress. We also tested whether the therapeutic efficacy of MSCs can be enhanced by FD treatment in a mouse model of cisplatin-induced AKI.

Materials and Methods

Cell Culture

Human MSCs from umbilical cord tissue were purchased from ATCC (Manassas, VA, USA). A total of three cell batches from different donors were used. MSCs were maintained in Minimum Essential Medium- α (MEM- α) (Thermo Fisher Scientific, Waltham, MA, USA) supplemented with 10% fetal bovine serum (Atlas Biologicals, Fort Collins, CO, USA) and antibiotics-antimycotics (Genedirex, Taoyuan, Taiwan). MSCs cultured for five or six passages were used in all experiments. FD was purchased from Sigma-Aldrich (St. Louis, MO, USA). First, MSCs were cultured with various concentrations of FD (1, 3, or 5 μ g/ml) for 24, 48, or 72 h. To evaluate the effect of FD on oxidative stress-induced cell death, FD (1 or 3 μ g/ml) was treated with MSCs in the presence of 300 μ M of hydrogen peroxide (Daejung Chemicals, Siheung-si, Korea) for 12, 24, or 48 h. Independently, MSCs prestimulated with 3 μ g/ml of FD for 72 h was treated either with 500 μ M

for 6 h (for assessing ROS generation and apoptosis) or with 300 μ M for 24 h (for measuring mitochondrial membrane potential). Cell viability was analyzed using a Cell Counting Kit-8 (CCK-8) (Dojindo Laboratories, Kumamoto, Japan) according to the manufacturer's instructions. The detailed procedures for the characterization of MSCs are available in the Supplemental Materials and Methods.

Quantitative Reverse Transcription PCR

Total RNA was extracted using TRIzol® (Invitrogen, Carlsbad, CA, USA) following the manufacturer's instructions. Complementary DNA (cDNA) was synthesized using a cDNA synthesis kit (Philekorea, Daejeon, Korea), and quantitative polymerase chain reaction (qPCR) was performed using an Accupower® 2 \times GreenStar qPCR Master Mix (Bioneer, Daejeon, Korea) in a CFX96 Touch Real-Time PCR Detection System (Bio-Rad Laboratories, Inc., Hercules, CA, USA). The expression of each gene was normalized against glyceraldehyde 3-phosphate dehydrogenase (GAPDH), and the relative expression was analyzed using the 2^{- $\Delta\Delta$ Ct} method²⁵. The sequences of the primers are as follows: GAPDH, 5'-GAGTCAACGGATTTGGTCGT-3' and 5'-TTGATTTGGAGGGATCTCG-3'; heme oxygenase-1 (HO-1), 5'-TCTCTGGCTGGCTTCCTTAC-3' and 5'-GCTTTTGGAGGTTTGAGACA-3'; and NRF2, 5'-TACCAGGTTGCCACA-3' and 5'-CATCTACAAACGGGAATGTCTGC-3'.

Analysis of Apoptosis

Apoptosis was measured using an Annexin V-FITC apoptosis detection kit (BD Biosciences, Franklin, NJ, USA). Briefly, MSCs were plated at a density of 1 \times 10⁵ cells/ml in six-well culture plates and incubated with or without FD for 72 h and then incubated with 500 μ M H₂O₂ for 6 h. The cells were then harvested, washed in cold phosphate-buffered saline (PBS), and resuspended in 500 μ l of binding buffer. Annexin V-FITC solution (5 μ l) and propidium iodide (5 μ l) were added to each group (100 μ l), and the cells were incubated for 30 min. Flow cytometry data were analyzed using the BD FACS DIVA software (Ver 6.1.3; BD Biosciences).

Detection of Mitochondrial Membrane Potential

After MSCs were stimulated with or without 3 μ g/ml of FD for 72 h, cells were treated with 300 μ M of hydrogen peroxide for 24 h. A JC-1 MitoMP Detection Kit (Dojindo Laboratories) was used to measure changes in mitochondrial membrane potential (MMP). Briefly, cells were washed with cold PBS, stained with 4 μ M JC-1, and incubated for 45 min at 37°C. Subsequently, the cells were washed twice with ice-cold PBS and analyzed using a BD FACSCanto™ II Cytometer and FACS DIVA software (Ver6.1.3; BD Biosciences).

Measurement of Reactive Oxygen Species

MSCs pretreated with or without FD (3 $\mu\text{g}/\text{ml}$) for 72 h were cultured with H_2O_2 (500 μM) for 6 h. Cells were then washed and incubated with 10 μM 2,7-dichlorofluorescein diacetate (DCF-DA; Sigma-Aldrich) for 30 min. After being washed twice with PBS, DCF fluorescence intensity (excitation/emission = 495/520 nm) was measured using a cell imaging system (Cytation5; BioTek, Winooski, VT, USA).

Western Blot Analysis

Cells were washed with ice-cold PBS, lysed using a radioimmunoprecipitation assay (RIPA) buffer (Bio-solution, Suwon, Korea), and centrifuged at $12,000 \times g$ for 15 min at 4°C . The protein concentration was then measured using a Pierce™ BCA Protein Assay Kit (Thermo Fisher Scientific). Protein extracts (20 μg) were separated by 10% sodium dodecyl sulfate-polyacrylamide gel electrophoresis and transferred to nitrocellulose membranes. The membrane was blocked with 5% non-fat dry milk in Tris-buffered saline with 0.1% Tween-20 (TBST) and incubated overnight at 4°C with primary antibodies against phosphorylated (p)-AKT1/2/3, AKT1/2/3, cAMP response element-binding protein (CREB), p-CREB, BAX, HO-1, and β -ACTIN. Detailed information on these antibodies is listed in Supplemental Materials and Methods. The membrane was then washed three times with TBST for 15 min each and incubated for 1 h at room temperature with horseradish peroxidase-conjugated anti-rabbit or anti-mouse antibodies (1:10,000) (Abcam, Cambridge, UK). The immunoreactivity of the blot was examined using an enhanced chemiluminescence kit (Thermo Fisher Scientific). The electrochemical images were then obtained using a Davinci-K Gel Imaging System (Davinci-K, Seoul, Korea). The relative densities of bands were quantified using ImageJ software (Version 1.50; National Institutes of Health, Bethesda, MD, USA).

Confocal Microscopic Analysis

Cells (7,000 per well) were plated in an eight-well chamber slide (SPL Lifesciences, Pochun, Korea) and cultured for 24 h. They were then washed three times with cold PBS and fixed using 4% paraformaldehyde in PBS (pH 7.4) for 10 min at room temperature. The cells were incubated for 10 min with PBS containing 0.1% Triton X-100 and washed three times with cold PBS, followed by blocking in 1% bovine serum albumin in PBST (PBS + 0.1% Tween20) for 30 min. The cells were then incubated with primary antibodies against NRF2 (Abcam; 1:1,000) overnight at 4°C . Cells were washed three times with cold PBS and then incubated with goat anti-rabbit IgG (Alexa Fluor® 488) (Abcam; 1:5,000) for 1 h. After the cells were washed three times with PBS, samples were stained with 0.1 $\mu\text{g}/\text{ml}$ 4',6-diamidino-2-phenylindole for 1 min. Images were analyzed and

recorded under a confocal microscope (Leica TCS SP8 STED; Leica Camera AG, Wetzlar, Germany).

Animal Studies

All animal experiments were approved by the Institutional Animal Care and Use Committee of Seoul National University (no. SNU-190413-6-1). Male BALB/c mice weighing 21–23 g (8 weeks old) were obtained from Koatech (Pyeongtaek, Korea) and maintained under specific pathogen-free conditions. The mice were randomly divided into several groups. Cisplatin (12 mg/kg) was intraperitoneally injected. After 24 h, MSCs (5×10^5) treated with or without FD (3 $\mu\text{g}/\text{ml}$) for 72 h were retro-orbitally injected. For negative control, saline was injected. All animals were euthanized by CO_2 asphyxiation at 96 h after cisplatin injection.

Serum Analysis

Blood was collected by cardiac puncture and left at room temperature for 20 min in a BD Microtainer Serum Separator Tube (BD Biosciences). After centrifugation at $3,000 \times g$ for 20 min, serum samples were subjected to measurement of blood urea nitrogen and creatinine using a Catalyst Dx Chemistry Analyzer system (IDEXX Laboratories, Inc., Westbrook, ME, USA). A tumor necrosis factor (TNF)- α kit was purchased from Abcam (ab208348, Mouse TNF alpha ELISA Kit; Abcam), and the concentrations were measured as described in the manufacturer's instructions.

Kidney Histology and Injury Scoring

Kidney tissues were fixed in 4% paraformaldehyde and processed for paraffin embedding. Sections were stained with hematoxylin and eosin for histological assessment. For quantification of renal injury, the injury score was analyzed as described in a previous study²⁶. Briefly, tubules were marked as viable (intact tubular morphology) or necrotic (totally disrupted tubule with loss of cuboidal cells) and counted in stained tissue at a $200\times$ magnification. With these two extremes, tubules with a thin cytoplasm containing less nuclei were counted as injured ones. Tubules showing more nuclei with normal cells were counted as recovering ones. Finally, the percentage (%) of each pattern in the total number of tubules was calculated.

Immunohistochemistry and TUNEL Assay

Formalin-fixed, paraffin-embedded slides were deparaffinized in xylene and rehydrated in descending order of ethanol (100%–70%). Then, antigen retrieval was performed using an Antigen Retrieval Buffer (Citrate Buffer pH 6.0) (Abcam) according to the manufacturer's instructions. An UltraVision LP Detection System HRP DAB kit (Thermo Fisher Scientific) was used according to the manufacturer's

protocol. Briefly, slides were immersed in UltraVision Hydrogen Peroxide Block for 10 min at room temperature, washed four times in PBST (0.05% Tween20), and incubated with UltraVision Protein Block for 5 min at room temperature. After washing four times with PBST, the slides were incubated with F4/80 (D2S9R) XP® Rabbit monoclonal antibody (mAb; 1:250) (70076T; Cell Signaling Technology, Danvers, MA, USA) and proliferating cell nuclear antigen (PCNA) mAb (1:500) (sc-56; SCBT, Dallas, TX, USA) overnight at 4°C. After washing in PBST four times, the reactivity was validated using a mouse/rabbit specific HRP/DAB IHC Detection Kit (Micro-polymer, ab236466; Abcam). The slides were then subsequently washed four times with distilled water and counterstained in Mayer's hematoxylin (4Science, Gyeonggi-do, Korea) for 1.5 min at room temperature. For detecting apoptotic cells in kidney tissues, TUNEL (terminal deoxynucleotidyl transferase dUTP nick end labeling) was performed using an ApopTag® Peroxidase *In Situ* Apoptosis Detection Kit (S7100; EMD Millipore, Temecula, CA, USA) according to the user guide. After washing in running tap water, the slides were dehydrated in ascending order of ethanol (from 70% to 100%). Images from representative fields were obtained using an Olympus BX43 light microscope (magnification, 400×; Olympus Corporation, Tokyo, Japan). Quantifications of positively stained cells were performed by calculating the mean number of positive cells from 10 non-overlapping fields per slide at a magnification of 400×.

Statistical Analysis

Statistical analysis was performed using analysis of variance, followed by Tukey's multiple comparisons test. All analyses were performed using GraphPad Prism 9.0 software (GraphPad, San Diego, CA, USA). $P < 0.05$ was considered statistically significant.

Results

Effect of FD on the Growth and Survival of MSCs

To determine the optimal concentration of FD for MSC proliferation, the growth of MSCs cultured under various concentrations of FD (0.1–50.0 µg/ml) was examined. As shown in Fig. 1A, the highest proliferation capacity of MSCs was observed when cultured under 0.5 and 1.0 µg/ml of FD at 48 and 72 h. Next, the effect of various concentrations of FD (1, 3, 5 µg/ml) on MSC proliferation was tested for 24, 48, and 72 h. At 24 h, the viability of MSCs was the highest when cultured under 3 µg/ml of FD. At 48 h, 1 and 3 µg/ml of FD showed an enhanced cell growth over 5 µg/ml. At 72 h, all concentrations of FD (1, 3, 5 µg/ml) led to an increase in cell growth to a similar degree (Fig. 1B). Based on these results, we selected 3 µg/ml as the concentration for all subsequent experiments. Next, we evaluated the potential of FD in

improving the survival of MSCs under oxidative stress. H₂O₂-induced oxidative cell death was observed at all time-points (12, 24, and 48 h). In contrast, the viability of MSCs was restored by FD treatment to a level comparable to that in cells in the steady state at 24 and 48 h (Fig. 1C).

As shown in Fig. 1D, AKT phosphorylation increased after 0.5 h of FD stimulation in MSCs. Rapid phosphorylation of CREB by the activation of the dopamine D1 receptor has been reported previously²⁷. Moreover, the CREB phosphorylation increased after 0.5 h of FD treatment but decreased to the baseline level at 1 h (Fig. 1E).

Characterization of FD-Treated MSCs

Both MSCs and FD-MSCs were positive for antibodies against CD73, CD90, and CD105, but negative for the hematopoietic/endothelial marker CD34 (Supplementary Fig. 1A). Next, we examined MSC and FD-MSC differentiation into chondrogenic, osteogenic, and adipogenic lineages. We found that the potential of differentiation toward these lineages increased in FD-MSCs compared with non-treated MSCs (Supplementary Fig. 1B; $P < 0.0001$ and $P = 0.012$ for chondrogenic and osteogenic differentiation, respectively). No difference was found in the adipogenic potential between MSCs and FD-MSCs (Supplementary Fig. 1B). Finally, FD-MSCs yielded more colony-forming units than observed with MSCs ($P = 0.006$; Supplementary Fig. 1C).

Effect of FD on NRF2/HO-1 Activation

Previous studies have revealed that the antioxidative effects of D1-like receptors are exerted by stimulating HO-1^{28,29}. Thus, we examined the effect of FD treatment on the expression of HO-1 and NRF2, two genes essential for antioxidative function. As shown in Fig. 2A, the messenger RNA expression of HO-1 was significantly higher in MSCs that received FD treatment for 72 h compared with the control (30-folds and 50-folds with 3 and 5 µg/ml FD, respectively) ($P < 0.0001$). In addition, the expression of NRF2, an upstream factor of HO-1, increased after 72 h of FD treatment ($P < 0.0001$ and $P = 0.0062$ at 3 and 5 µg/ml FD, respectively). Furthermore, immunoblot analysis revealed that HO-1 protein expression increased in FD-MSCs compared with the control (Fig. 2B, $P = 0.0202$). Finally, nuclear translocation of NRF2 was observed after FD treatment (Fig. 2C), indicating that FD reduces oxidative cell death via NRF2/HO-1 pathway activation³⁰.

Effect of FD on MSC Apoptosis

Figure 3A illustrates the overall experimental design for investigating the anti-apoptotic function of FD in MSCs undergoing oxidative cell death. We assessed the effect of FD on BAX stabilization and subsequently on oxidative stress-induced apoptosis of MSCs (Fig. 3B). Immunoblot analysis

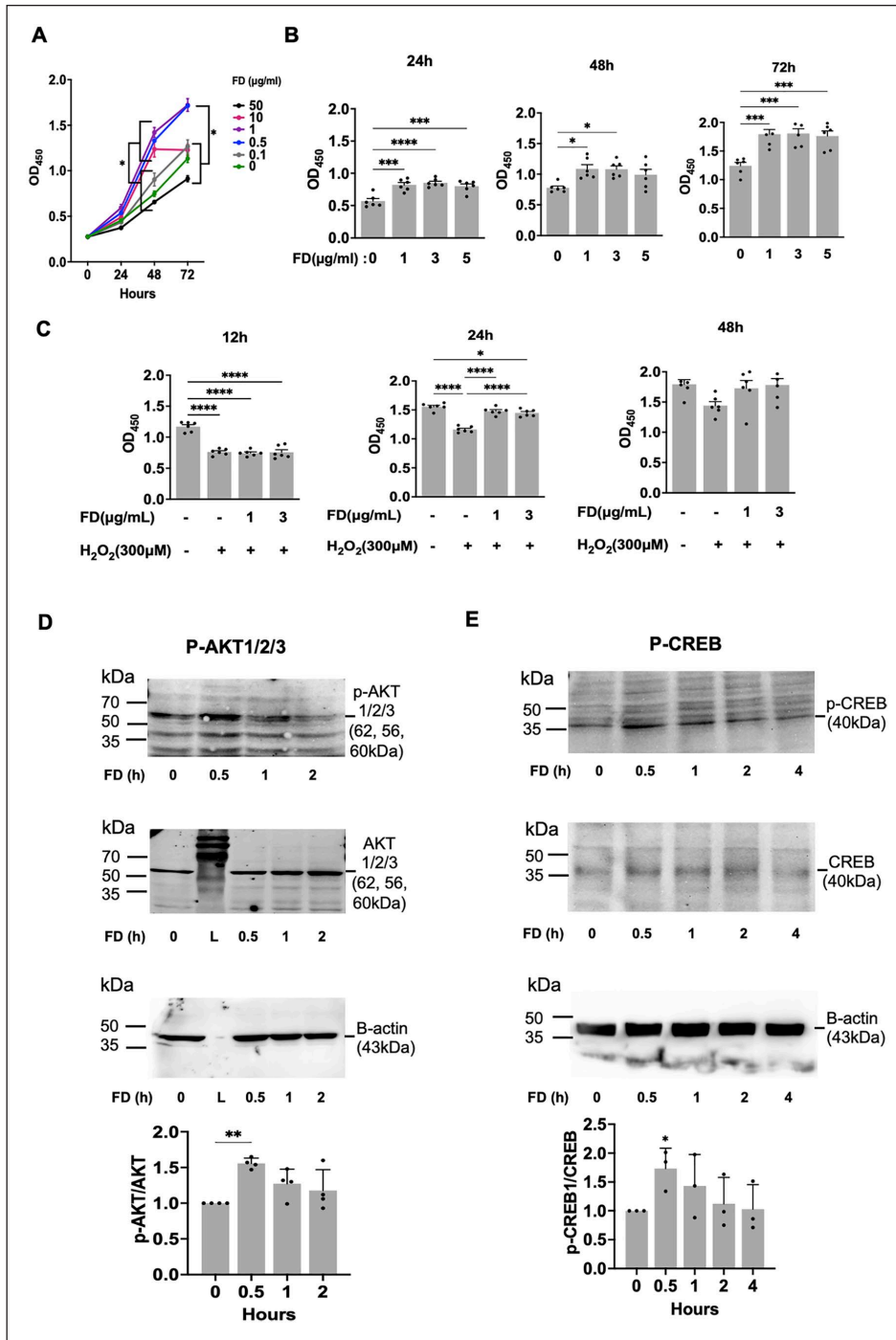


Figure 1. Effect of fenoldopam mesylate (FD) on the growth and oxidative stress-induced cell death in mesenchymal stem cells (MSCs). (A) Growth kinetics of MSCs treated with various concentrations of FD for 72 h. Optical density (OD₄₅₀) was measured for determining the relative number of viable cells after 3 h of Cell Counting Kit-8 (CCK-8) treatment. (B) Effect of various concentrations of FD on the growth of MSCs. The relative number of viable cells under various concentrations of FD was determined by measuring the optical density (OD₄₅₀) after 3 h of CCK-8 treatment. (C) Effect of FD on the survival of MSCs under H₂O₂-mediated cell death. MSCs were pretreated with FD (1 or 3 μg/ml) in the presence or absence of H₂O₂ for 12, 24, and 48 h. (D and E) Immunoblot analysis of AKT (D) and cAMP response element-binding protein (CREB) (E) phosphorylation in MSCs stimulated with FD (3 μg/ml). Beta-actin was used as the loading control. The expression of phosphorylated AKT and CREB was normalized against those of total AKT and CREB, respectively. Data are expressed as mean ± standard deviation. **P* < 0.05; ***P* < 0.01; ****P* < 0.001; *****P* < 0.0001.

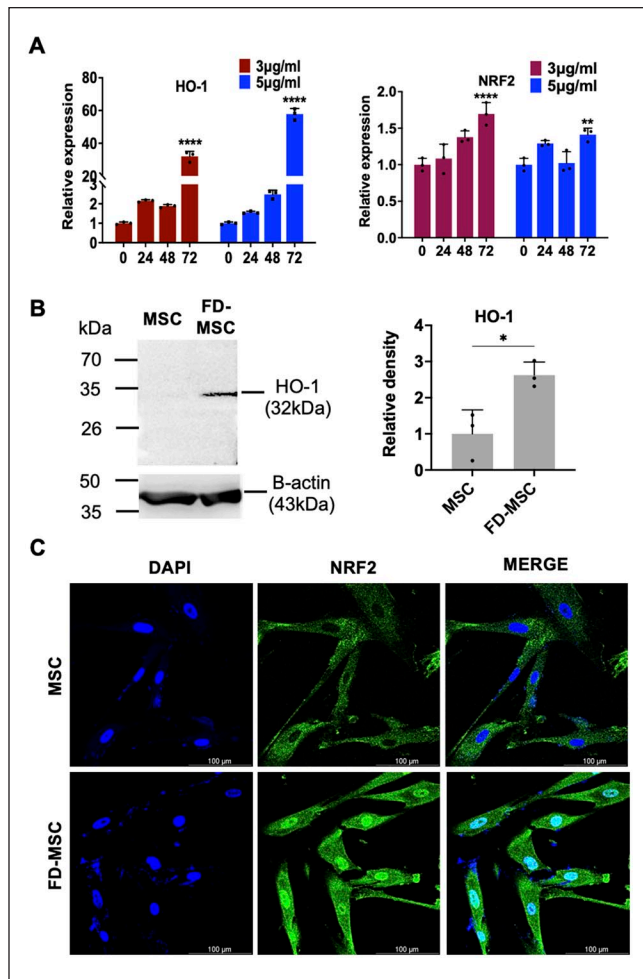


Figure 2. Effect of fenoldopam mesylate (FD) treatment on nuclear factor erythroid-2-related factor 2 (NRF2)/heme oxygenase-1 (HO-1) expression in mesenchymal stem cells (MSCs). (A) Quantitative reverse transcription polymerase chain reaction analysis of HO-1 and NRF2 messenger RNA expression in MSCs treated with FD (3 or 5 µg/ml) for various durations. **** $P < 0.0001$ and ** $P = 0.0062$. (B) Immunoblot analysis of HO-1 expression in MSCs treated with or without FD (3 µg/ml) for 24 h. Beta-actin was used as the loading control. * $P = 0.0202$. (C) Immunocytochemical analysis of nuclear NRF2 expression in MSCs treated with or without FD (3 µg/ml) for 24 h. Data are expressed as mean \pm standard deviation.

revealed that H_2O_2 upregulated the stabilization of proapoptotic BAX, whereas FD treatment remarkably downregulated its expression. Accumulation of reactive oxygen species (ROS) beyond the cells' scavenging capacity decreases the MMP, which leads to apoptotic cell death through decreased ATP production^{31,32}. As shown in Fig. 3C, H_2O_2 considerably reduced MMP, while FD increased the MMP to a level comparable to that of the untreated control group.

We next investigated whether FD can reduce apoptotic cell death induced by ROS. Flow cytometry analysis revealed that the relative population of viable cells was decreased by

ROS (80% and 58% in normal and H_2O_2 -treated cells, respectively), while FD treatment led to a recovery of cell viability to a degree comparable to that of the normal control (Fig. 3D). Next, we examined whether pretreatment of MSCs with FD can reduce the generation of ROS under oxidative stress. As shown in Fig. 3E, ROS generation was increased by H_2O_2 , but markedly reduced by FD treatment. Collectively, these data suggest that FD protects oxidative cell death via BAX stabilization, increasing MMP, inhibiting apoptosis, and reducing ROS production.

Assessment of the Therapeutic Function of FD-MSCs in AKI Mice

As shown in Fig. 4A, the color of the kidney of the AKI mice turned pale. FD-MSCs led to a restoration to dark purple, while this change was less significant in the kidney from the MSC-treated mice. The level of blood urea nitrogen (BUN) and creatinine was markedly lower in the FD-MSC animals than in the MSC-treated animals ($P = 0.0027$ and 0.0209 , respectively). Furthermore, cisplatin treatment led to an increase in the serum level of TNF- α , which was reversed by FD-MSCs ($P = 0.0053$). However, this change was not observed with MSCs ($P = 0.1863$). We next compared the degree of tubular damage of AKI mice that received MSCs or FD-MSCs. To this end, we classified the degree of tubular damage into healthy, recovering, injured, and necrotic, based on a previous protocol²⁶. Then, we measured the relative percentages of tubules of each category. In vehicle-treated animals, the percentage of injured (17.4%, $P < 0.0001$) or necrotic (19.1%, $P = 0.0001$) tubules was higher than for recovering ones (2.2%). In the MSC-treated group, the percentage of injured (12.7%, $P = 0.0005$) or necrotic (10.7%, $P = 0.0029$) tubules was higher than for recovering ones (6.4%). In contrast, less necrotic tubules (4.4%) were detected compared with recovering (9.5%, $P = 0.0005$) or injured (7.9%, $P = 0.0005$) tubules. No difference was found in the percentage of recovering and injured cells in animals that received FD-MSCs.

We found more PCNA-positive cells in the AKI mice compared with the normal animals ($P = 0.007$). This increase was augmented in the mice administered MSCs ($P = 0.0012$ compared with the vehicle), and this increase was more significant in FD-MSCs ($P < 0.0001$ compared with the vehicle). In addition, the number of PCNA-positive cells was more abundant in FD-MSCs compared with MSCs ($P < 0.0001$) (Fig. 5A). As shown in Fig. 5B, the TUNEL analysis showed that the number of apoptotic cells markedly increased in the renal tissue of the AKI mice. In the MSC-treated animals, the number of apoptotic cells remained unchanged. In the FD-MSC-treated animals, however, the number of apoptotic cells significantly reduced compared with that in animals that received the vehicle ($P = 0.0212$). No significant change was observed between the animals that received

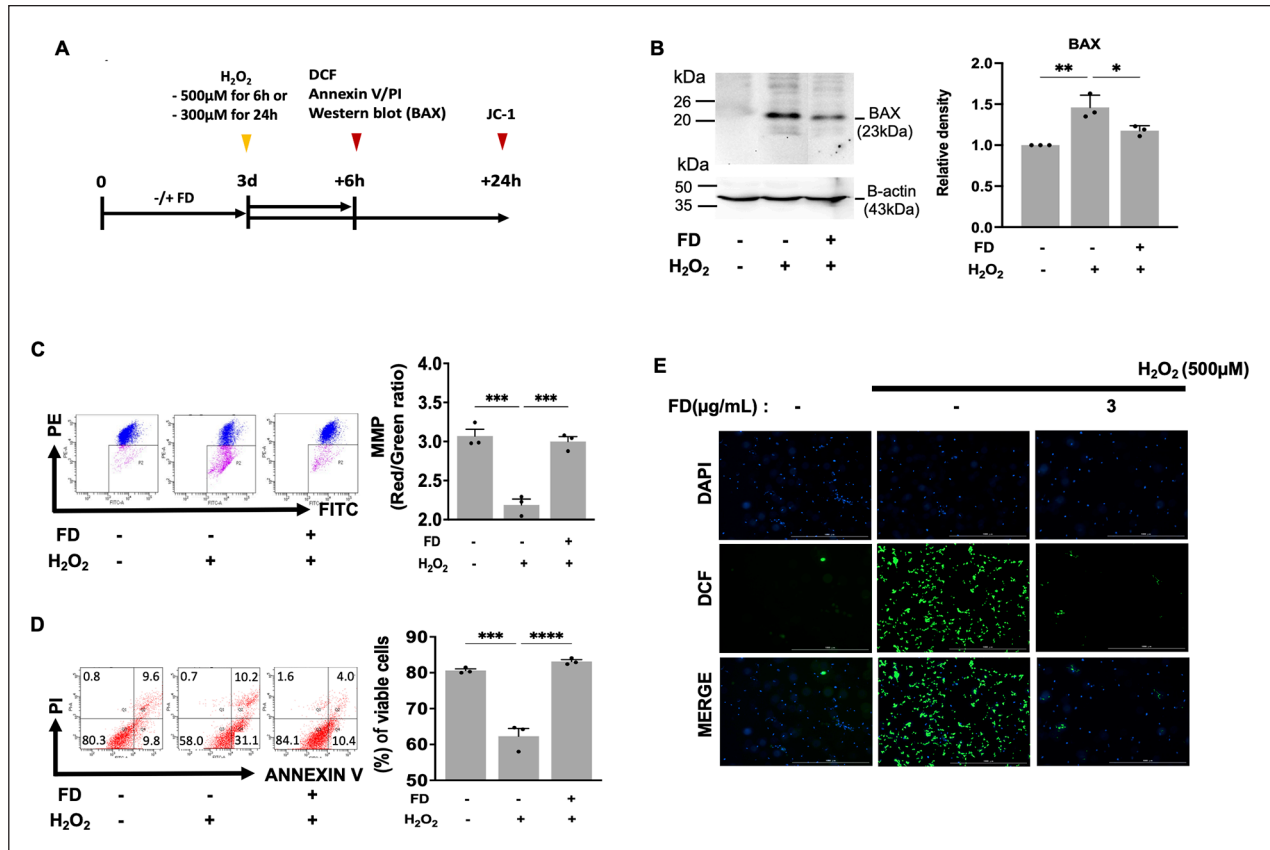


Figure 3. Role of fenoldopam mesylate (FD) on apoptotic cell death of mesenchymal stem cells (MSCs). (A) Schematic illustration of the experimental design. MSCs were cultured with or without FD (3 μ g/ml) for 72 h. Subsequently, MSCs were incubated with 300 or 500 μ M of H₂O₂ for 24 or 6 h, respectively. JC-1 dye (tetraethylbenzimidazolylcarbocyanine iodide) was used for detecting mitochondrial membrane potential (MMP). (B) Immunoblot analysis of BAX in MSCs and FD-MSCs. The lanes were rearranged from a single blot that includes other lanes tested with various concentrations of H₂O₂ (300, 500, and 700 μ M). Beta-actin was used as the loading control. (C) Analysis of MMP (Ψ m) in MSCs and FD-MSCs undergoing oxidative stress. The change in MMP was measured by calculating the ratio between red and green fluorescence (R/G) measured by flow cytometry. (D) Flow cytometry analysis of reactive oxygen species (ROS)-mediated apoptosis in MSCs pretreated with or without FD. (E) Detection of ROS in MSCs and FD-MSCs. ROS was detected by H₂DCFH-DA (2',7'-dichlorodihydrofluorescein diacetate) assay. Magnifications are 40 \times . Data are expressed as mean \pm standard deviation. * P < 0.05; ** P < 0.01; *** P < 0.001.

MSCs and FD-MSCs ($P = 0.4872$). Finally, macrophage infiltration decreased in the MSC- and FD-MSC-treated mice ($P = 0.0021$ and $P < 0.0001$, respectively) compared with the vehicle control. Notably, less F4/80-stained cells were detected in the animals treated with FD-MSCs compared with the animals treated with MSC ($P = 0.0002$) (Fig. 5C).

Discussion

The purpose of this study was to evaluate whether FD, a dopamine D1 receptor agonist, can improve the antioxidative and anti-apoptotic functions in MSCs undergoing oxidative stress and to assess whether FD-treated MSCs have superior function over nontreated MSCs in improving AKI. We found that FD-MSCs had improved potential in self-renewal activity, osteogenic/cardiogenic differentiation, and proliferation via CREB and AKT phosphorylation. In addition, FD

stimulated NRF2/HO-1 expression and nuclear translocation of NRF2. The prosurvival role of FD in MSCs was further supported by a reduction in BAX expression, ROS generation, and apoptotic cell death, as well as an increase in the MMP in MSCs under oxidative injury. In the mouse model of AKI, FD-MSC was more effective at enhancing the renal function, histological score, macrophage infiltration, and tubular cell proliferation and decreasing apoptosis compared with non-treated MSCs. Our results suggest that FD can serve as a novel priming factor that can enhance the therapeutic outcome in MSC-based therapy in AKI.

Dopamine D1 receptor belongs to the superfamily of G protein-coupled receptors¹⁹. In the kidneys, a local dopaminergic system regulates blood pressure, electrolyte balance, and kidney function^{19,33}. FD has been approved for clinical use, and its downstream signaling pathways are well identified²⁰, making it readily usable as a cell culture supplement.

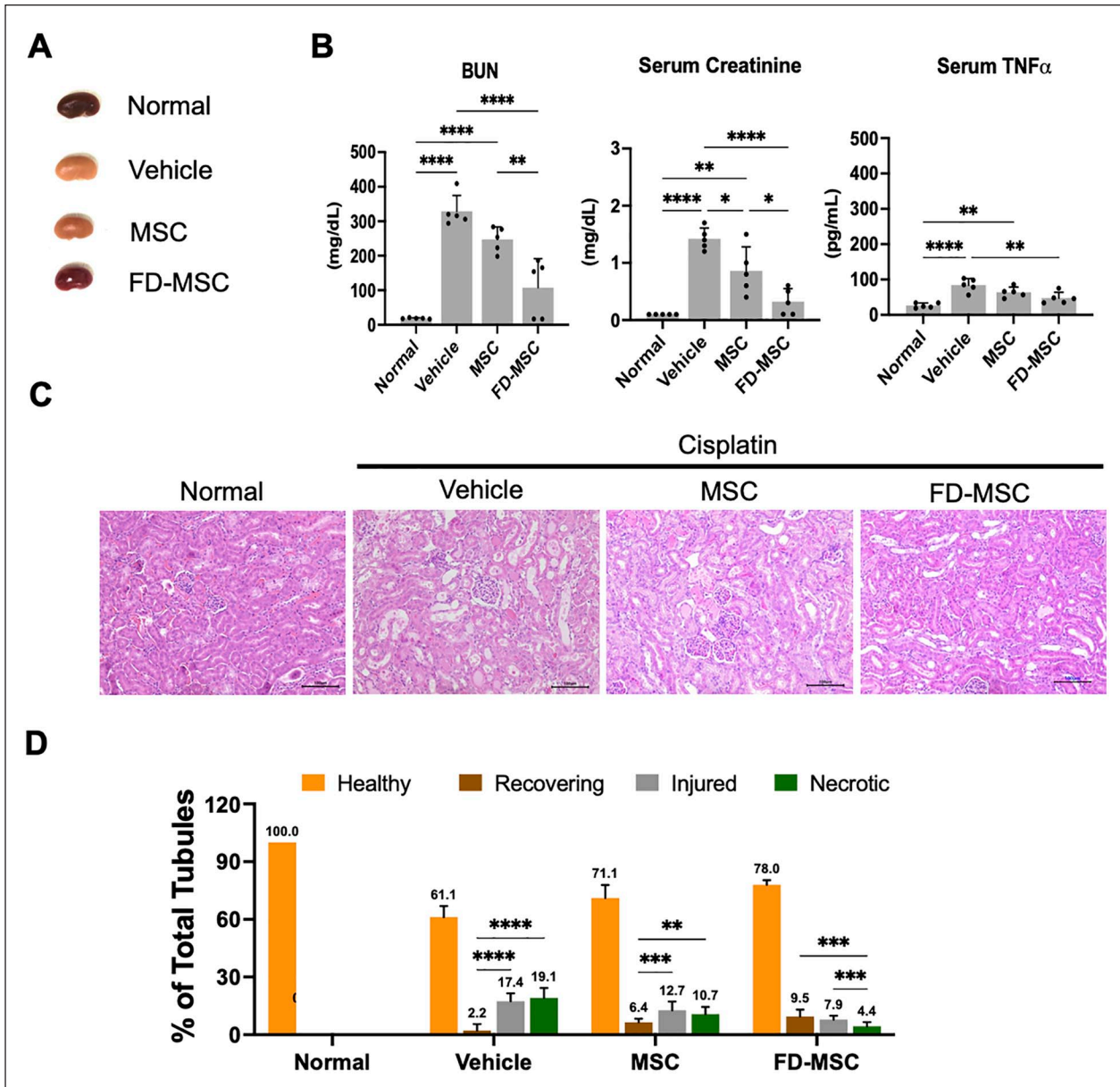


Figure 4. Evaluation of the therapeutic efficacy of fenoldopam mesylate (FD)-treated mesenchymal stem cells (FD-MSCs) in acute kidney injury (AKI). MSCs were treated with or without FD (3 μ g/ml) for 72 h. At 24 h of cisplatin administration, MSCs or FD-MSCs were intravenously administered into the AKI mice. At 96 h, mice were sacrificed and various parameters were analyzed. Animals administered saline were used as the control. (A) The morphology and color of kidneys. (B) The serum concentration of blood urea nitrogen (BUN) (** P = 0.0027 between MSCs and FD-MSCs), creatinine (* P = 0.029, MSC vs FD-MSC), and tumor necrosis factor- α (** P = 0.0053, vehicle vs FD-MSC). (C) Assessment of renal injury by microscopic image of hematoxylin and eosin-stained renal tissues. (D) Measurement of renal injury. More injured (P < 0.0001) and necrotic (P = 0.0001) tubules over recovering ones were found in vehicle-treated mice. In MSC-treated animals, more injured (** P = 0.0005) and necrotic (** P = 0.0029) tubules over recovering ones were found. In FD-MSC-treated mice, the proportion of necrotic (** P = 0.0005) or injured (** P = 0.0005) tubules was decreased compared with recovering ones. All data are expressed as mean \pm standard deviation. Five mice were used in each group. * P < 0.05; ** P < 0.01; *** P < 0.001; **** P < 0.0001.

A previous study showed that FD can exert a cytotoxic effect by increasing the production of ROS³⁴. Accordingly, we first determined the optimal concentration of FD. We found that at a concentration of 3 μ g/ml, FD did not alter the basic characteristics of MSCs, but augmented their growth,

differentiation, and colony-forming ability and restored apoptotic cell death induced by oxidative stress. Moreover, we found that FD activates CREB, which is consistent with a previous study which reported that FD stimulates adenylate cyclase and subsequent CREB activation³⁵. In addition, FD

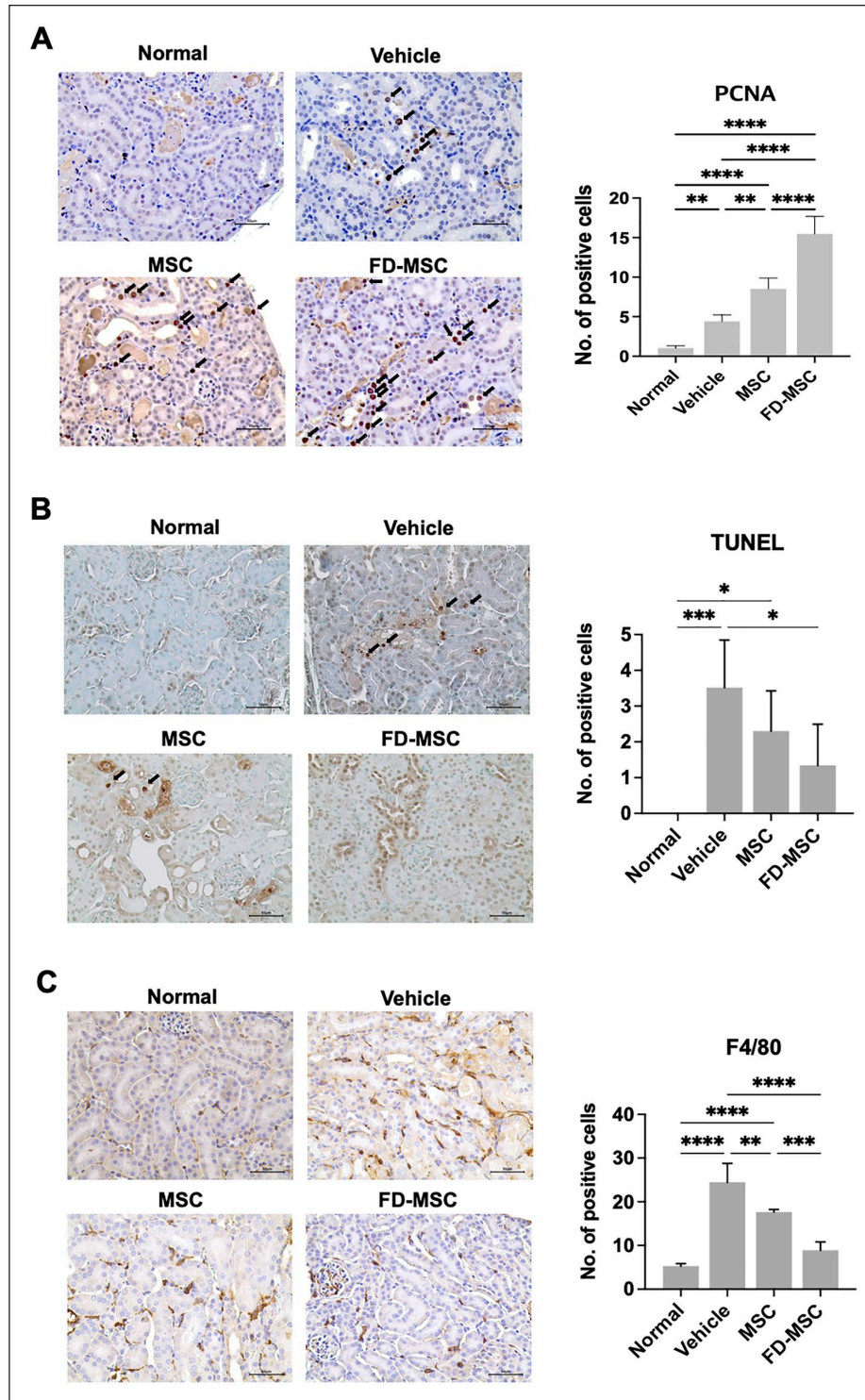


Figure 5. Immunohistochemical staining of kidneys from acute kidney injury mice. Tissues were obtained after 72 h of cell or vehicle transplantation. (A) Expression of proliferating cell nuclear antigen (PCNA). $P = 0.007$, vehicle vs normal; $P = 0.0012$, mesenchymal stem cell (MSC) vs normal; $P < 0.0001$, FD-treated MSC (FD-MSC) vs normal. (B) Detection of apoptotic tubules. $P = 0.0212$, vehicle vs FD-MSC; $P = 0.4872$, MSC vs FD-MSC. (C) Detection of F4/80-positive cells in renal tissue. $P = 0.0021$, MSC vs vehicle; $P < 0.0001$, MSC vs FD-MSC. Quantifications were performed by calculating the number of positively stained cells in 10 fields per slide at a magnification of 400 \times . All data are expressed as mean \pm standard deviation. Five mice were used in each group. Scale bar is 50 μ m. * $P < 0.05$; ** $P < 0.01$; *** $P < 0.001$; **** $P < 0.0001$.

activated AKT signaling, which is a well-known pathway for migration, survival, and growth of MSCs³⁶. FD treatment promoted the nuclear translocation of NRF2, which may have increased the upregulation of its downstream gene HO-1. It is well known that cells have developed endogenous cytoprotective strategies to recover from damage caused by excessive ROS; the NRF2/antioxidant response element (ARE) axis is a powerful antioxidative mechanism for regulating the redox state, contributing to homeostasis against intracellular oxidative stress^{30,37}. As an ARE-regulated phase II detoxifying enzyme, HO-1 is upregulated by NRF2 activation, and NRF2/HO1 has an antioxidative function³⁸. Determining changes in the downstream metabolites of HO-1, such as bilirubin or carbon monoxides, which have been reported to have anti-apoptotic function, would be necessary to clarify its function^{30,39}.

The therapeutic efficacy of MSCs can be increased by altering the culture conditions or by being treated with soluble factors via improving adhesion, migration, and survival and reducing premature senescence¹⁰. For example, the expression of glucose-regulated protein 78 (GRP78), a key regulator of unfolded protein response, has been stabilized in MSCs cultured under hypoxic conditions, promoting GRP78-activated AKT signaling, resulting in enhanced MSC survival when transplanted in the legs of mice undergoing hindlimb ischemia⁴⁰. Although preconditioning is ideal for improving the survival or therapeutic function of MSCs, finding a proper substrate can be challenging; only a few studies have shown the effect of MSCs preconditioned with chemical compounds or cytokines. Zhou et al.⁴¹ showed that erythropoietin, a glycoprotein hormone produced by the kidney, can increase the expression of SIRT1 and BCL2 in MSCs, thus reducing the apoptosis and increasing the localization of MSCs in the kidney of rats that received ischemia/reperfusion injury. Another potent, clinically available biological substance is melatonin, a neurohormone secreted by the pineal gland. Recent studies have demonstrated that melatonin is able to reduce free radicals as well as local inflammation. In a model of AKI induced by cecal-ligation and puncture, treatment of MSCs with melatonin showed considerably greater therapeutic effects induced by antioxidation, anti-inflammation, anti-apoptosis, and anti-fibrosis activity⁴². Zhao et al.⁴³ reported that conditioned medium collected from adipose-derived stem cells pretreated with melatonin lead to an increased proliferation of human renal epithelial cells (HK-2) and reduced apoptotic cell death induced by cisplatin.

The enhanced therapeutic outcome of FD-MSCs may substantially be due to increased HO-1 expression. Indeed, a substantial amount of literature have demonstrated that HO-1 plays a pivotal role in inhibiting the mechanisms of tissue injury that are associated with inflammation, oxidative stress, and ischemia/reperfusion injury⁴⁴. In AKI, several studies have demonstrated that HO-1 is related to inhibiting the progression of AKI induced by nephrotoxin,

ischemia/reperfusion injury, and rhabdomyolysis^{44,45}. Cho et al.⁴⁶ demonstrated that human adipose tissue-derived MSCs cultured for four passages have a higher HO-1 level; in addition, coculture of HO-1^{high} MSCs with HK-2 undergoing cisplatin-induced death leads to an increased survivability compared with MSCs with other lower level passages. Our preliminary examination showed that the number of injected cells in the kidney of AKI mice was similar between MSCs and FD-MSCs after 72 h (data not included), indicating that FD does not affect the long-term survivability of MSCs *in vivo*. From these results, the effect of FD on MSC may be largely due to the antioxidative function of HO-1.

MSCs and FD-MSCs further augmented the number of PCNA-stained cells that were increased by cisplatin, with FD-MSCs showing an improved outcome. The increase in PCNA-positive cells with cisplatin is consistent with previous studies that used various experimental renal injuries, including D-galactose-induced oxidative stress in the kidney, as well as cisplatin- or ischemia/reperfusion-induced AKI⁴⁷⁻⁴⁹. Given the therapeutic function of MSC in tissue regeneration⁵⁰, the increase in PCNA-positive cells in FD-MSC over MSC may be due to enhanced survival. This possibility is supported by a previous investigation that showed an increase in KI-67-positive cells by MSCs in a cisplatin-induced AKI model in mice⁵¹ and a dose-dependent increase in PCNA-stained cells by quercetin in the kidney of a D-galactose-induced oxidative stress model in rats⁴⁷. Another study showed that the stromal vascular fraction from adipose tissue transplanted into renal subcapsular space markedly increases the KI67-positive cells in a rat model of cisplatin-induced AKI while reducing apoptotic cell death⁵². Collectively, it can be argued that the increased therapeutic outcome by FD-MSCs over MSCs is possibly due to the proliferation of tubular cells in cisplatin-induced AKI.

We found that FD-MSCs had an improved anti-inflammatory potential, as shown by reduced macrophage infiltration into the AKI kidney as well as the serum level of TNF- α . Several reports have shown that macrophage infiltration is a major cellular mechanism for inflammation in renal diseases, including AKI^{50,53}. Together with the results of PCNA staining, a marked reduction in the number of infiltrated macrophages by FD-MSCs over MSCs is likely to be associated with reduced tubular cell death by FD-MSCs as seen in the TUNEL staining, as well as enhancement of renal function markers and the injury score. These findings are in line with other studies. For example, Zheng et al.⁵⁰ demonstrated that the mobilization of macrophages into the kidney is suppressed upon treatment with conditioned medium of MSCs following unilateral ureteral obstruction in mice. Furthermore, the infiltration of macrophages into the kidney was increased in the AKI mice, which was reduced by genistein, a soybean-derived flavonoid. Finally, the reduced level of serum TNF- α may have contributed to the amelioration of AKI by FD-MSCs, and this notion can be supported by a review⁵⁴ and previous studies. For example, Ramesh and Reeves⁵⁵

showed that TNF- α is a key player in AKI induced by cisplatin, as shown by reduced AKI progression in mice deficient in TNF- α or those treated with anti-TNF- α -antibody. Collectively, these results suggest that the enhanced recovery of AKI by FD-MSc is at least attributable to reduced inflammation by FD treatment.

In summary, our findings suggest that FD augments the survival and therapeutic function of MSCs in an oxidative environment. Our results may provide an efficient method for preparing robust therapeutic MSCs for AKI.

Acknowledgments

We thank the staff of Designed Animal Research Center, Institutes of Green Bio Science & Technology, Seoul National University, for technical support during tissue preparation and animal care.

Author Contributions

S.Y.K., H.J.C., and T.M.K. conducted experiments and analyzed the data. S.Y.K. and H.J.C. interpreted the data. S.Y.K. and T.M.K. wrote the manuscript.

Ethical Approval

This study was approved by the Institutional Animal Care and Use Committee (IACUC) of Seoul National University, Seoul, Korea (approval number: SNU-190413-6-1).

Statement of Human and Animal Rights

All procedures involving animal experiments were carried out in accordance with animal care and use committee guidelines of Seoul National University, Korea.

Statement of Informed Consent

Informed consent for using human cells was not applicable because the cells were obtained commercially.

Declaration of Conflicting Interests

The author(s) declared no potential conflicts of interest with respect to the research, authorship, and/or publication of this article.

Funding

The author(s) disclosed receipt of the following financial support for the research, authorship, and/or publication of this article: This work was supported by a National Research Foundation of Korea (NRF) grant funded by the Korean government (MSIT) (2021R1A2C2093867). This research was supported by Korean Fund for Regenerative Medicine funded by Ministry of Science and ICT, and Ministry of Health and Welfare (22C0610L1-11), Republic of Korea.

ORCID iDs

Hye Jin Cho  <https://orcid.org/0000-0003-1804-117X>

Tae Min Kim  <https://orcid.org/0000-0003-0015-2701>

Supplemental Material

Supplemental material for this article is available online.

References

1. Abdelaziz TS, Fouda R, Hussin WM, Elyamny MS, Abdelhamid YM. Preventing acute kidney injury and improving outcome in critically ill patients utilizing risk prediction score (PRAIOC-RISKS) study. A prospective controlled trial of AKI prevention. *J Nephrol*. 2020;33(2):325–34.
2. Susantitaphong P, Cruz DN, Cerda J, Abulfaraj M, Alqahtani F, Koulouridis I, Jaber BL, Acute Kidney Injury Advisory Group of the American Society of Nephrology. World incidence of AKI: a meta-analysis. *Clin J Am Soc Nephrol*. 2013;8(9):1482–93.
3. Khwaja A. KDIGO clinical practice guidelines for acute kidney injury. *Nephron Clin Pract*. 2012;120(4):c179–84.
4. Li JS, Li B. Renal injury repair: how about the role of stem cells. *Adv Exp Med Biol*. 2019;1165:661–70.
5. Gonsalez SR, Cortês AL, Silva RCD, Lowe J, Prieto MC, Silva Lara LD. Acute kidney injury overview: from basic findings to new prevention and therapy strategies. *Pharmacol Ther*. 2019; 200:1–12.
6. Waikar SS, Liu KD, Chertow GM. Diagnosis, epidemiology and outcomes of acute kidney injury. *Clin J Am Soc Nephrol*. 2008;3(3):844–61.
7. Ghannam S, Bouffi C, Djouad F, Jorgensen C, Noel D. Immunosuppression by mesenchymal stem cells: mechanisms and clinical applications. *Stem Cell Res Ther*. 2010;1(1):2.
8. Yun CW, Lee SH. Potential and therapeutic efficacy of cell-based therapy using mesenchymal stem cells for acute/chronic kidney disease. *Int J Mol Sci*. 2019;20(7):1619.
9. Pan B, Fan G. Stem cell-based treatment of kidney diseases. *Exp Biol Med (Maywood)*. 2020;245(10):902–10.
10. Ocansey DKW, Pei B, Yan Y, Qian H, Zhang X, Xu W, Mao F. Improved therapeutics of modified mesenchymal stem cells: an update. *J Transl Med*. 2020;18(1):42.
11. Wang M, Yuan Q, Xie L. Mesenchymal stem cell-based immunomodulation: properties and clinical application. *Stem Cells Int*. 2018;2018:3057624.
12. Galipeau J, Sensebe L. Mesenchymal stromal cells: clinical challenges and therapeutic opportunities. *Cell Stem Cell*. 2018; 22(6):824–33.
13. Moll G, Ankrum JA, Kamhieh-Milz J, Bieback K, Ringdén O, Volk HD, Geissler S, Reinke P. Intravascular mesenchymal stromal/stem cell therapy product diversification: time for new clinical guidelines. *Trends Mol Med*. 2019;25(2):149–63.
14. Caplan H, Olson SD, Kumar A, George M, Prabhakara KS, Wenzel P, Bedi S, Toledano-Furman NE, Triolo F, Kamhieh-Milz J, Moll G, et al. Mesenchymal stromal cell therapeutic delivery: translational challenges to clinical application. *Front Immunol*. 2019;10:1645–15.
15. Amiri F, Jahanian-Najafabadi A, Roudkenar MH. In vitro augmentation of mesenchymal stem cells viability in stressful microenvironments: in vitro augmentation of mesenchymal stem cells viability. *Cell Stress Chaperones*. 2015;20(2): 237–51.
16. Cruz FF, Rocco PR. Hypoxic preconditioning enhances mesenchymal stromal cell lung repair capacity. *Stem Cell Res Ther*. 2015;6:130.

17. Hu C, Li L. Preconditioning influences mesenchymal stem cell properties in vitro and in vivo. *J Cell Mol Med.* 2018;22(3):1428–42.
18. Alfadda AA, Sallam RM. Reactive oxygen species in health and disease. *J Biomed Biotechnol.* 2012;2012:936486.
19. Olivares-Hernandez A, Figuero-Perez L, Cruz-Hernandez JJ, Gonzalez Sarmiento R, Usategui-Martin R, Miramontes-Gonzalez JP. Dopamine receptors and the kidney: an overview of health- and pharmacological-targeted implications. *Biomolecules.* 2021;11(2):254.
20. Murphy MB, Murray C, Shorten GD. Fenoldopam: a selective peripheral dopamine-receptor agonist for the treatment of severe hypertension. *N Engl J Med.* 2001;345(21):1548–57.
21. Yasunari K, Kohno M, Kano K, Minami M, Yoshikawa J. Dopamine as a novel antioxidative agent for rat vascular smooth muscle cells through dopamine D1-like receptors. *Circulation.* 2000;101:2302–8.
22. Li H, Han W, Villar VA, Keever LB, Lu Q, Hopfer U, Quinn MT, Felder RA, Jose PA, Yu P. D1-like receptors regulate NADPH oxidase activity and subunit expression in lipid raft microdomains of renal proximal tubule cells. *Hypertension.* 2009;53(6):1054–61.
23. Yu Y, Wang JR, Sun PH, Guo Y, Zhang ZJ, Jin GZ, Zhen X. Neuroprotective effects of atypical D1 receptor agonist SKF83959 are mediated via D1 receptor-dependent inhibition of glycogen synthase kinase-3 beta and a receptor-independent anti-oxidative action. *J Neurochem.* 2008;104(4):946–56.
24. Li GY, Li T, Fan B, Zheng YC, Ma TH. The D₁ dopamine receptor agonist, SKF83959, attenuates hydrogen peroxide-induced injury in RGC-5 cells involving the extracellular signal-regulated kinase:p38 pathways. *Mol Vis.* 2012;18:2882–95.
25. Livak KJ, Schmittgen TD. Analysis of relative gene expression data using real-time quantitative PCR and the 2^{-ΔΔCT} Method. *Methods.* 2001;25(4):402–8.
26. Hesketh EE, Czopek A, Clay M, Borthwick G, Ferenbach D, Kluth D, Hughes J. Renal ischaemia reperfusion injury: a mouse model of injury and regeneration. *J Vis Exp.* 2014;88:51816.
27. Liu FC, Graybiel AM. Spatiotemporal dynamics of CREB phosphorylation: transient versus sustained phosphorylation in the developing striatum. *Neuron.* 1996;17(6):1133–44.
28. Armando I, Villar VA, Jose PA. Dopamine and renal function and blood pressure regulation. *Compr Physiol.* 2011;1(3):1075–1117.
29. George LE, Lokhandwala MF, Asghar M. Novel role of NF-kappaB-p65 in antioxidant homeostasis in human kidney-2 cells. *Am J Physiol Renal Physiol.* 2012;302(11):F1440–46.
30. Loboda A, Damulewicz M, Pyza E, Jozkowicz A, Dulak J. Role of Nrf2/HO-1 system in development, oxidative stress response and diseases: an evolutionarily conserved mechanism. *Cell Mol Life Sci.* 2016;73(17):3221–47.
31. Rigoulet M, Yoboue ED, Devin A. Mitochondrial ROS generation and its regulation: mechanisms involved in H₂O₂ signaling. *Antioxid Redox Signal.* 2011;14(3):459–68.
32. Brand MD, Buckingham JA, Esteves TC, Green K, Lambert AJ, Miwa S, Murphy MP, Pakay JL, Talbot DA, Echtay KS. Mitochondrial superoxide and aging: uncoupling-protein activity and superoxide production. *Biochem Soc Symp.* 2004(71):203–13.
33. Cuevas S, Villar V, Jose P, Armando I. Renal dopamine receptors, oxidative stress, and hypertension. *Int J Mol Sci.* 2013;14(9):17553–72.
34. Cosentino M, Rasini E, Colombo C, Marino F, Blandini F, Ferrari M, Samuele A, Lecchini S, Nappi G, Frigo G. Dopaminergic modulation of oxidative stress and apoptosis in human peripheral blood lymphocytes: evidence for a D1-like receptor-dependent protective effect. *Free Radic Biol Med.* 2004;36(10):1233–40.
35. Undieh AS. Pharmacology of signaling induced by dopamine D₁-like receptor activation. *Pharmacol Ther.* 2010;128(1):37–60.
36. Chen J, Crawford R, Chen C, Xiao Y. The key regulatory roles of the PI3K/Akt signaling pathway in the functionalities of mesenchymal stem cells and applications in tissue regeneration. *Tissue Eng Part B Rev.* 2013;19(6):516–28.
37. Itoh K, Wakabayashi N, Katoh Y, Ishii T, Igarashi K, Engel JD, Yamamoto M. Keap1 represses nuclear activation of anti-oxidant responsive elements by Nrf2 through binding to the amino-terminal Neh2 domain. *Genes Dev.* 1999;13(1):76–86.
38. Alam J, Stewart D, Touchard C, Boinapally S, Choi AM, Cook JL. Nrf2, a Cap'n'Collar transcription factor, regulates induction of the heme oxygenase-1 gene. *J Biol Chem.* 1999;274(37):26071–78.
39. Balla G, Jacob HS, Balla J, Rosenberg M, Nath K, Apple F, Eaton JW, Vercellotti GM. Ferritin: a cytoprotective antioxidant strategem of endothelium. *J Biol Chem.* 1992;267(25):18148–53.
40. Lee JH, Yoon YM, Lee SH. Hypoxic preconditioning promotes the bioactivities of mesenchymal stem cells via the HIF-1alpha-GRP78-Akt axis. *Int J Mol Sci.* 2017;18(6):1320.
41. Zhou S, Qiao YM, Liu YG, Liu D, Hu JM, Liao J, Li M, Guo Y, Fan LP, Li LY, others. Bone marrow derived mesenchymal stem cells pretreated with erythropoietin accelerate the repair of acute kidney injury. *Cell Biosci.* 2020;10(1):130.
42. Chen HH, Lin KC, Wallace CG, Chen YT, Yang CC, Leu S, Chen YC, Sun CK, Tsai TH, Chen YL, Chung SY, et al. Additional benefit of combined therapy with melatonin and apoptotic adipose-derived mesenchymal stem cell against sepsis-induced kidney injury. *J Pineal Res.* 2014;57(1):16–32.
43. Zhao J, Young YK, Fradette J, Eliopoulos N. Melatonin pretreatment of human adipose tissue-derived mesenchymal stromal cells enhances their prosurvival and protective effects on human kidney cells. *Am J Physiol Renal Physiol.* 2015;308(12):F1474–83.
44. Nath KA. Heme oxygenase-1: a provenance for cytoprotective pathways in the kidney and other tissues. *Kidney Int.* 2006;70(3):432–43.
45. Tracz MJ, Alam J, Nath KA. Physiology and pathophysiology of heme: implications for kidney disease. *J Am Soc Nephrol.* 2007;18(2):414–20.
46. Cho HS, Jang HN, Jung MH, Jang SJ, Jeong S-H, Lee TW, Bae E, Chang S-H, Park DJ, Kim JH. The protective effect of human adiposederived mesenchymal stem cells on cisplatin-induced nephrotoxicity is dependent on their level of expression of heme oxygenase-1. *Eur J Inflamm.* 2020;18:1–11.
47. El-Far AH, Lebda MA, Noreldin AE, Atta MS, Elewa YHA, Elfeky M, Mousa SA. Quercetin attenuates pancreatic and renal D-galactose-induced aging-related oxidative alterations in rats. *Int J Mol Sci.* 2020;21(12):4348.

48. Stroo I, Stokman G, Teske GJ, Raven A, Butter LM, Florquin S, Leemans JC. Chemokine expression in renal ischemia/reperfusion injury is most profound during the reparative phase. *Int Immunol*. 2010;22(6):433–42.
49. Miyaji T, Kato A, Yasuda H, Fujigaki Y, Hishida A. Role of the increase in p21 in cisplatin-induced acute renal failure in rats. *J Am Soc Nephrol*. 2001;12(5):900–908.
50. Zheng J, Wang Q, Leng W, Sun X, Peng J. Bone marrow-derived mesenchymal stem cell-conditioned medium attenuates tubulointerstitial fibrosis by inhibiting monocyte mobilization in an irreversible model of unilateral ureteral obstruction. *Mol Med Rep*. 2018;17(6):7701–707.
51. Morigi M, Imberti B, Zoja C, Corna D, Tomasoni S, Abbate M, Rottoli D, Angioletti S, Benigni A, Perico N, Alison M, et al. Mesenchymal stem cells are renoprotective, helping to repair the kidney and improve function in acute renal failure. *J Am Soc Nephrol*. 2004;15(7):1794–804.
52. Yasuda K, Ozaki T, Saka Y, Yamamoto T, Gotoh M, Ito Y, Yuzawa Y, Matsuo S, Maruyama S. Autologous cell therapy for cisplatin-induced acute kidney injury by using non-expanded adipose tissue-derived cells. *Cytotherapy*. 2012;14(9):1089–1100.
53. Sung MJ, Kim DH, Jung YJ, Kang KP, Lee AS, Lee S, Kim W, Davaatseren M, Hwang JT, Kim HJ, Kim MS, et al. Genistein protects the kidney from cisplatin-induced injury. *Kidney Int*. 2008;74(12):1538–47.
54. Akcay A, Nguyen Q, Edelstein CL. Mediators of inflammation in acute kidney injury. *Mediators Inflamm*. 2009;2009:137072.
55. Ramesh G, Reeves WB. TNF-alpha mediates chemokine and cytokine expression and renal injury in cisplatin nephrotoxicity. *J Clin Invest*. 2002;110(6):835–42.